Transverse Instability in the ATF Damping Ring

Eun-San Kim
High Energy Accelerator Research Organization (KEK)
1-1 Oho, Tsukuba, Ibaraki, 305, Japan

Abstract

To understand the behaviors of the transverse instability in the ATF damping ring, a multiparticle tracking simulation was performed in the presence of the transverse and longitudinal wake fields which were induced by rf cavities. The features of transverse instabilities with dependence on chromaticities and suppression of these instability by modulating chromaticity were shown.

1 Introduction

The beam current is often limited by coherent instabilities. These instabilities can occur either in the longitudinal or in the transverse motions. Longitudinal ones often cause bunch lengthening or an increase of the loss rate. Here we discuss transverse instabilities of single beam since we have been studied longitudinal instabilities in the past[1].

When chromaticity is zero, the strong head-tail instability occurs in the particles's transverse motion. This instablity has a threshold which depends on bunch current, longitudinal and transverse wake fields, and betatron and synchrotron tunes. The beam's size blows up above the threshold current. When chromaticity is not zero, both the strong head-tail and the head-tail instabilities occur in the particles's transverse motion.

The simulations were performed with the purpose to understand transverse instability in the ATF damping ring. We investigate the instability by using multiparticle tracking. The simulations describe the motions of single beam in the presence of the transverse and the longitudinal wake fields which are induced by two rf cavities in the ATF damping ring. The simulations on transverse instabilities in ATF damping ring does not show mode mixing, and show beam enlargement and beam blow-up. In this paper, we discuss these properties of transverse instability which has dependence on chromaticity in ATF damping ring.

T. Nakamura proposed concept of varying chromaticity to suppress the head-tail instability[2]. W. Cheng et.al. also showed analytical and numerical study of the suppression of the transverse head-tail instability by modulating the chromaticity over a synchrotron period[3]. Here we apply the same concept to the machine of ATF damping ring and show results of suppression of the head-tail instability.

The paper is organized in the following way. In Sec.2, the motions of macroparticle tracking for the simulation are described. In Sec.3, longitudinal and transverse wakefields by rf cavities in the ATF damping ring are given. In Sec.4, we describe the results of

the simulation and then give a qualitative discussions on the transverse instability in the ATF damping ring.

2 Macroparticle Motion

To describe the electron's motion in a damping ring we use a standard multiparticle tracking method. The phase space distribution of the beam is represented by N_p macroparticles. The beam is expected to be Gaussain with a mean energy, mean bunch length, mean transverse beam sizes whch are equal to zero. The initial coordinates of macroparticles are chosen to have these expected properties. A simulation was performed for ATF damping ring with 3000 macroparticles and the parameters in ATF damping ring are listed in Table I. Macroparticles are tracked in phase space with equations of motion which include radiation damping and exciation, synchrotron and betatron oscillations, and transverse and longitudinal wakefields.

In tracking of longitudinal motion, each macroparticle i has position and energy coordinates (z_i, ε_i). The longitudinal motion of a macroparticle i on revolution number n are derived from its coordinated on turn $n-1$[1][4][5]:

$$\varepsilon_i(n) = \varepsilon_i(n-1) - \frac{2T_o}{\tau_d}\varepsilon_i(n-1) + 2\sigma_{\varepsilon o}\sqrt{\frac{T_o}{\tau_d}}r_{1i}(n) + V'_{rf}z_i(n-1) + W(z_i)(n) \quad (1)$$

$$z_i(n) = z_i(n-1) + \frac{\alpha c T_o}{E_o}\varepsilon_i(n), \quad (2)$$

with r_{1i} is Gaussain random number with mean 0 and rms standard deviation 1. The slope of the rf voltage (a negative quantity) is given by

$$V'_{rf} = 2\pi\nu_{rf}\hat{V}[1-(U_o/\hat{V})^2]^{1/2}. \quad (3)$$

The symbols in equations (1) -(3) are defined in Table 1. A macroparticle i is affected by the wakefields of all macroparticles which precede it in the bunch. The wakefield $W(z_i)$ is a function of the longitudinal displacement of macroparticle i as well as the macroparticles which precede it. The macroparticles are tracked at the beginning of the rf cavity and we track the macroparticles for 2 longitudinal damping times. $\nu_{so}T_o$ and τ_d/T_o are given by 242 turns and 43272 turns.

In tracking of transverse motion, each macroparticle i has horizontal and vertical positions (x and y), and slopes of their positions (x' and y'). The equations of motion in transverse coordinates are

$$\begin{aligned} x_i(n) = {} & M_{11}[\varepsilon_i(n)]x_i(n-1) + M_{12}[\varepsilon_i(n)]x'_i(n-1)(1-\frac{T_o}{\tau_x}) \\ & + \sqrt{\frac{2\epsilon_z\beta_x T_o}{\tau_x}}r_{2i}(n) + M_{12}[\varepsilon_i(n)]\frac{W_i^x(n-1)}{E_o}, \end{aligned} \quad (4)$$

and

$$x_i'(n) = M_{21}[\varepsilon_i(n)]x_i(n-1) + M_{22}[\varepsilon_i(n)]x_i'(n-1)(1-\frac{T_o}{\tau_x})$$
$$+\sqrt{\frac{2\epsilon_z T_o}{\beta_x \tau_x}} r_{3i}(n) + M_{22}[\varepsilon_i(n)]\frac{W_i^x(n-1)}{E_o}, \tag{5}$$

where r_{2i} and r_{3i} are Gaussain random number with mean 0 and rms 1. Here x denotes horizontal and vertical coordinates. The symbols in these equations are also defined in Table 1. In the horizontal W_i^x is independent of the horizontal coordinate of a macroparticle i and dependent of the horizontal coordinates of the macroparticles that precede it

Defining the chromaticity ξ as

$$\xi = \frac{dQ_x/Q_x}{\varepsilon/E_o} \tag{6}$$

The transfer matrix in transverse motion is given by

$$M(\varepsilon) = \begin{pmatrix} \cos 2\pi Q_x(\varepsilon), & \beta_x \sin 2\pi Q_x(\varepsilon) \\ -1/\beta_x \sin 2\pi Q_x(\varepsilon), & \cos 2\pi Q_x(\varepsilon) \end{pmatrix}, \tag{7}$$

where β_x is the betatron function at the position of rf cavity, and $Q_x(\varepsilon)$ is the energy dependent tune

$$Q_{\beta_x}(\varepsilon) = Q_{\beta_x}(0)(1+\xi\varepsilon/E_o). \tag{8}$$

It is important to point out in this simulation that there is no coupling between horizontal and vertical betatron motions. The longitudinal displacement affects transverse motions because transverse wakefields are a function of the longitudinal displacement.

Table-1: Parameters of the ATF Damping Ring used in this simulation

Beam Energy	E_o	1.3 GeV
Cicumference	L	138.6 m
Energy Spread	$\sigma_{\epsilon o}$	$5.467e^{-4}$
Bunch Length	σ_{zo}	6.8 mm
RF Frequency	ν_{rf}	714 MHz
Harmonic number	h	330
RF Voltage	$\hat{V}_{rf}$	0.22 MV
Revolution Frequency	f_{rf}	2.164 MHz
Synchrotron frequency	ν_{so}	8.95 KHz
Momentun Compaction	α	0.00195
Damping Time	τ_x, τ_y, τ_d	17 ms, 27ms, 20ms
Revolution Period	T_o	460 ns
Betatron Tune	Q_x, Q_y	15.145, 8.715
Beta Function at Cavity	β_x, β_y	13.35 m, 11.97 m
Emittance	ϵ_x, ϵ_y	$5e^{-9}$ m, $5e^{-11}$m
Synchrotron Tune	ν_s	4.1×10^{-3}
Synchrotron Radiation Loss	U_o	155 keV

3 Wakefield

Collective effects are given by the wakefield. We need Green function wake of the damping ring in order to study instabilities. However, it suffices if we can obtain the wakefield of a bunch that is very short compared to the natural bunch length in the ring, and that has been calculated out to a sufficient distance behind the driving bunch. For our wake function, using the code ABCI, we calculated the wake potential of a 1 mm Gaussain bunch for two rf cavities in the ATF damping ring. These longitudinal and transverse wake potentials are shown in Figure 1. Here, the parts on front of bunch center ($z < 0$) were discarded.

To calculate wakefields, we binned the macroparticles in z without smoothing. The wakefields on any turn are given by

$$W_{ind}(z) = -eN \sum_{i=1}^{n} n_i W_L(z_i - z_n) \tag{9}$$

$$W_{ind}(x) = -eN \sum_{i=1}^{n} x_i W_T(z_i - z_n), \tag{10}$$

with N the bunch population and n_i is number of macroparticles in the i bin and x_i is transverse displacements of the macroparticles in the i bin. $W_L(z_i - z_n)$ and $W_T(z_i - z_n)$ are the longitudinal and transverse wake functions, respectively.

$$W_L(0) = \frac{1}{2} \lim_{z \to 0^+} W_L(z)$$

and

$$W_T(0) = 0.$$

In each turn we use 680 bins extending over $5\sigma_z$.

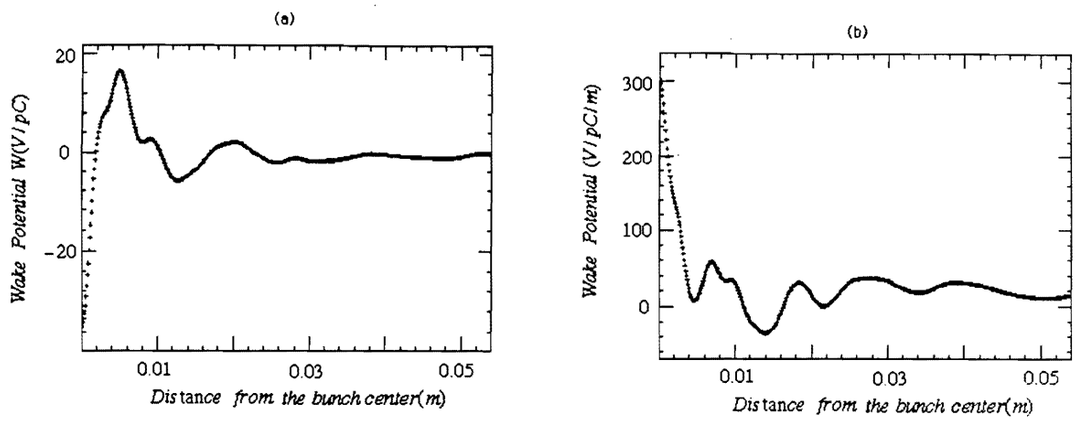

Figure 1: (a) longitudinal and (b) transverse wake potentials for two cavities in ATF damping ring. The charge bunch is a Gaussain with an rms of 1mm. The parts on front of bunch center ($z < 0$) were discarded.

4 Qualitative results for ATF Damping ring

4.1 Transverse instability at zero chromaticity

The nature of the instability is shown in Figure 2. The zero chromaticity instability is evident in both the rms center-of-mass motion and the beam size. The rms center-of-mass motion is defined as:

$$\sigma_{\bar{x}}^2(n) = \frac{1}{2N_s+1} \sum_{i=n-N_s}^{i=n+N_s} \bar{x}^2(i),$$

where $\bar{x}(i)$ is the mean position on turn i

$$\bar{x}(i) = \frac{1}{N_p} \sum_{m=1}^{N_p} x_m(i),$$

N_s is the integer part of $1/\nu_s$. The rms beam size is defined as

$$\sigma^2(n) = \frac{1}{N_p} \sum_{m=1}^{N_p} [x_m(n) - \bar{x}(n)]^2.$$

In this paper, rms center-of-mass motion and rms beam size normalized by nominal beam size will be plotted.

The Figure 2.(a) and (b) show the the vertical and horizontal center-of-mass motions for the beam currents of 3.4 mA, 10.2 mA and 20.4 mA, respectively. They show the contribution of the instability to center-of-mass motion as the beam currents increase.

The Figure 2.(c) shows the vertical beam sizes for the beam currents of 3.4 mA, 10.2 mA and 20.4 mA. The vertical beam sizes are increased as the beam currents increase. However, the horizontal beam sizes showed natural beam size. On the other hand, above beam current 27 mA, it was shown that both horizontal and vertical beam sizes grow dramatically.

At zero chromaticity the vertical beam size is in more lower beam currents enlarged than horizontal beam size. Above beam current 27 mA, the horizontal beam size grows

more dramatically than vertical beam size. That is, the beam sizes show enlargement and blow-up as beam currents increase.

A fast Fourier Transform of the mean position $\bar{x}(n)$ shows the tunes of the dominant modes. Figure 3 shows features of the tune shifts as a function of currents for a 6.8 mm bunch length. Figure 3.(a) shows the fast Fourier Transform of the mean horizontal position of the beam for several beam currents. This shows that m=0 mode $[Q(I=0)=Q_\beta]$ has shifted to higher tunes as the beam currents increase. We note that m=-1 mode $[Q(I=0)=Q_\beta-Q_s]$ and m=+1 mode $[Q(I=0)=Q_\beta+Q_s]$ have not been shown clearly. Figure 3.(b) shows the fast Fourier Transform of the mean vertiacl position of the beam. This shows that m=0 mode has shifted to lower tunes as the beam currents increase. We can see m=+1 mode and m=-1 mode as the beam currents increase. However, it was not shown that the m=0 mode has shifted sufficiently to mix with the m=-1 mode by 61.2 mA.

There is no indication of the instability being mode mixing between m=0 mode and m=-1 mode. Examination of the FFT and the growth in beam size lead to the conclusion that at zero chromaticity the beam current is limited by the stability of the m=0 mode.

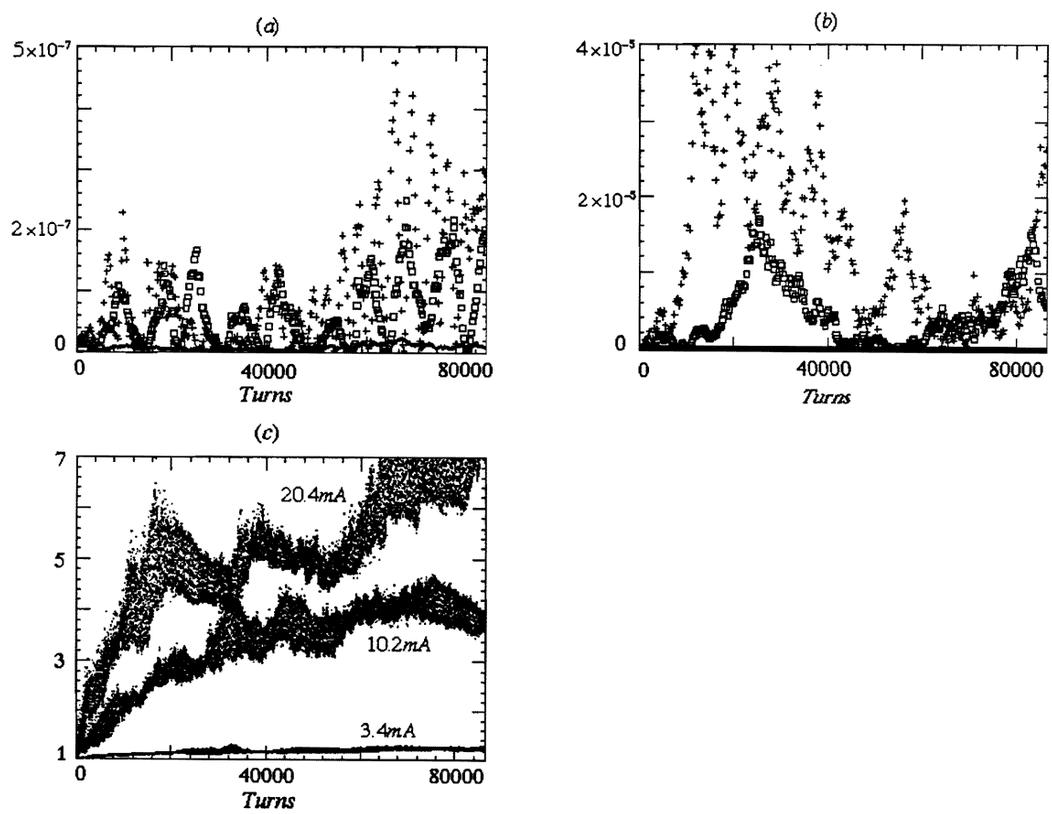

Figure 2: The zero chromaticity instability. (a) and (b) show the vertical and horizontal center-of-mass motions, respectively. (c) shows the vertical beam sizes. In (a) and (b), point, cross and square symbols represent transverse postions of center-of-mass motion for currents of 3.4 mA, 10.2 mA and 20.4 mA, respectively.

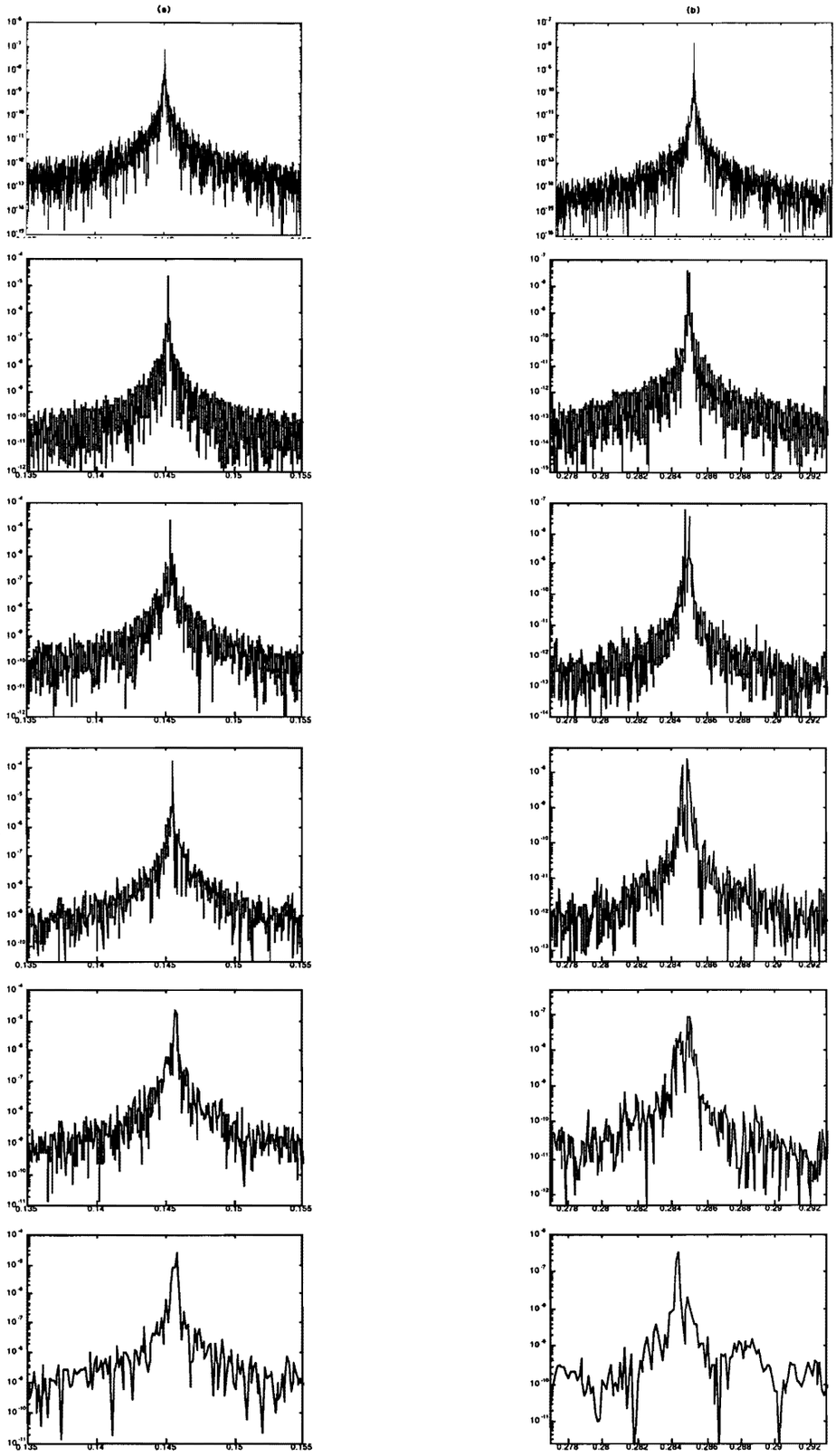

Figure 3: Fast Fourier Transforms of the mean horizontal (left figures) and vertical (right figures) positions of the beam. Q_x=0.145, Q_y=0.285 and ν_s=4.1 $\times 10^{-3}$.

4.2 Transverse instabilities at non-zero chromaticity

We will see the head-tail effect occuring at positive chromaticity. Figure 4.(a) and (b) show the rms horizonal and vertical beam sizes for the values of positive chromaticity ξ=0.1 and ξ=0.3 in beam current of 10.2 mA, respectively. The beam sizes increase with increasing positive chromaticity. All particles in the bunch move in phase resulting in growing size of beam.

Figure 4.(c) and (d) show the horizonal and vertical center-of-mass motions for the values of positive chromaticity ξ=0.1 and ξ=0.3 in beam current of 10.2 mA, respectively. They show that the instability is also evident in the center-of-mass motion.

The horizontal beam size and horizontal center-of-mass motion grow more dramatically than vertical beam size and vertical center-of mass-motion if once beam size blows up. This behavior shows the same feacture as zero chromaticity does. At ξ=0.1, it was shown that beam blows up dramatically above 18mA.

Figure 5.(a) shows the fast Fourier Transform of the mean horizontal position of the beam for several beam currents in ξ=0.1. This shows that m=0 mode has shifted to higher tunes as the beam currents increase. We note that m=-1 mode and m=+1 mode have been shown clearly. Figure 5.(b) shows the fast Fourier Transform of the mean vertical positions of the beam for ξ=0.1. This shows that m=0 mode has shifted to lower tunes as the beam currents increase. We can also see m=+1 mode and m=-1 mode. However, it was not shown that the m=0 mode has shifted sufficiently to mix with the m=-1 mode by 61.2 mA.

We also note that at ξ=0.1, there is no indication of the instability being mode mixing between m=0 mode and m=-1 mode. Examination of the FFT and the growth in beam size lead to the conclusion that at ξ=0.1 the beam current is limited by the stability of the m=0 mode.

4.3 Transverse Instabilities at varying chromaticity

Here we consider a method to suppress transverse head-tail instability by means of variation of the chromaticity[2][3]. The concept is to introduce incoherent tune spread inside a beam by modulating the chromaticity by synchrotron frequency. We assume that the chromaticity ξ which is modulated by the synchrotron frequency w_s is varied as

$$\xi(t) = \xi_o + \xi_1 cos w_s t, \tag{11}$$

which is no longer a constant of time t and w_s is the synchrotron angular frequency. The constant part of the chromaticity, ξ_o, causes the head-tail instability. This incoherent tune spread is not effective in stabilizing the head-tail instability. The ξ_1 is introduced to generate an incoherent tune spread that suppresses the head-tail instability.

Figure 6.(a) and (b) show the horizontal and vertical center-of-mass motions for ξ_o=0.2 and ξ_1=0, respectively. Figure 6.(c) and (d) show the horizontal and vertical center-of-mass motions for ξ_o=0.2 and ξ_1=0.2, respectively.

Figure 7 shows the fast Fourier Transforms of the mean transverse positions of the beam in 10.2 mA. (a) and (b) show for horizontal and vertical in ξ_o=0.2, ξ_1=0, respectively. (c) and (d)) for horizontal and vertical in ξ_o=0.2, ξ_1=0.2, respectively. We can also see that the instability does not occur in (c) and (d) by introduction of varying chromaticity.

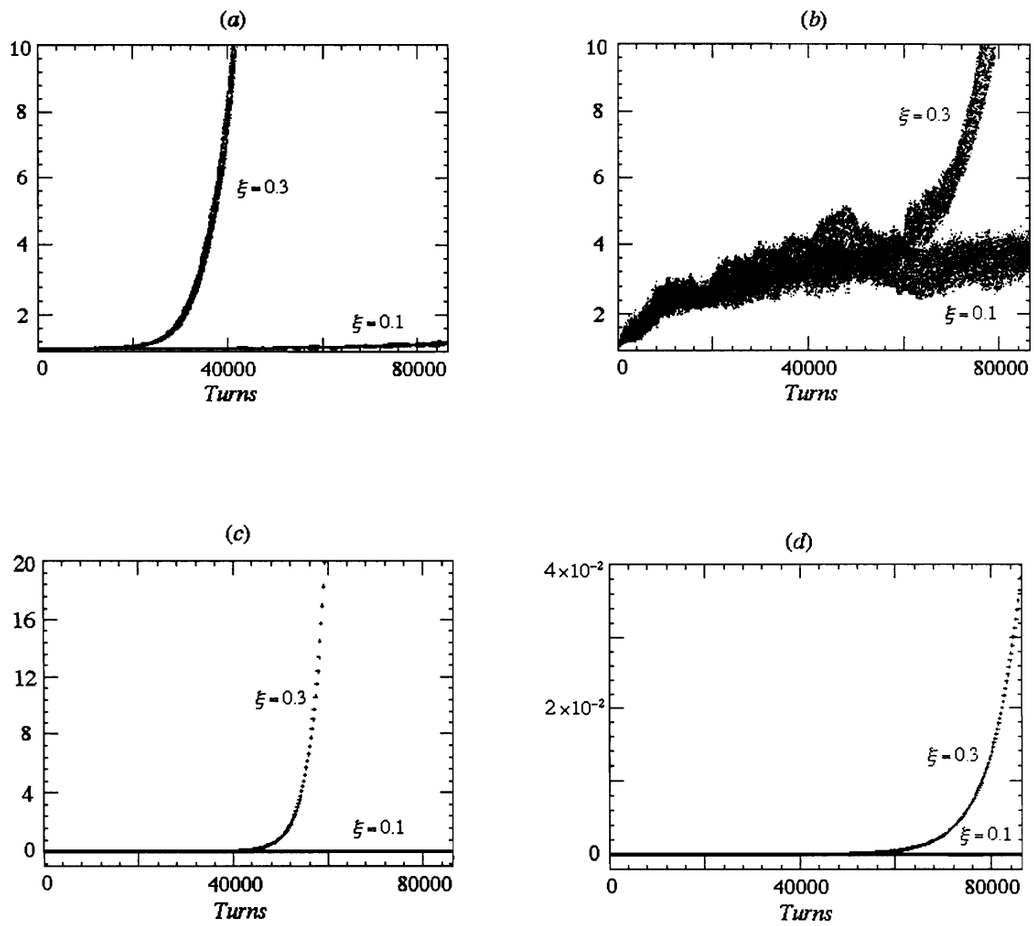

Figure 4: Chromaticity dependent instability at positive chromaticity ξ=0.1 and ξ=0.3. (a) and (b) show the horizontal and vertical beam sizes, respectively. (c) and (d) show the horizontal and vertical center-of-mass motion, respectively.

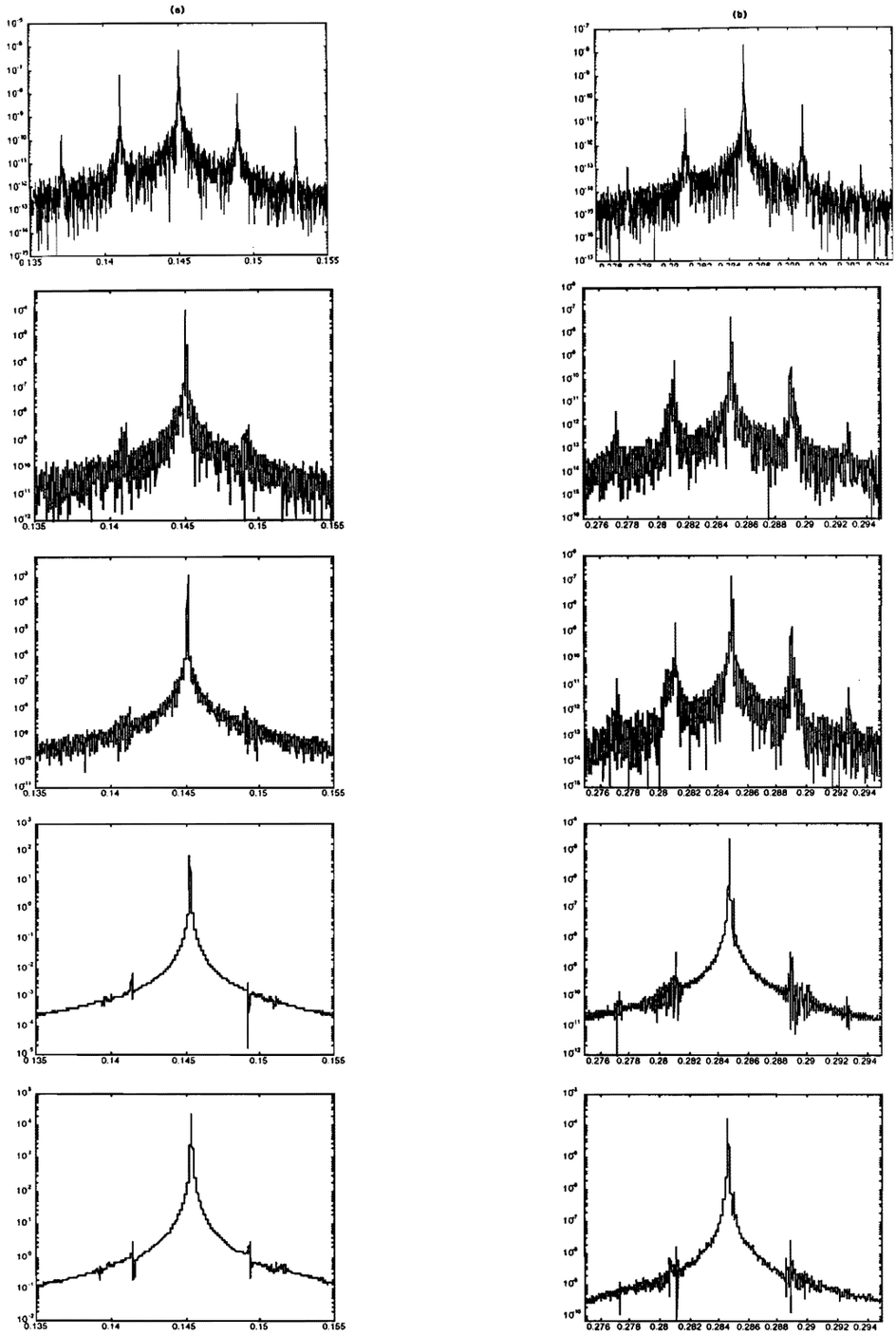

Figure 5: Fast Fourier Transforms of the mean horizontal (a) and vertical (b) positions of the beam. The betatron tune and the betatron tune plus and minus the synchrotron tune are shown. The chromaticity ξ is 0.1. Q_x=0.145, Q_y=0.285 and ν_s=4.1 $\times 10^-3$.

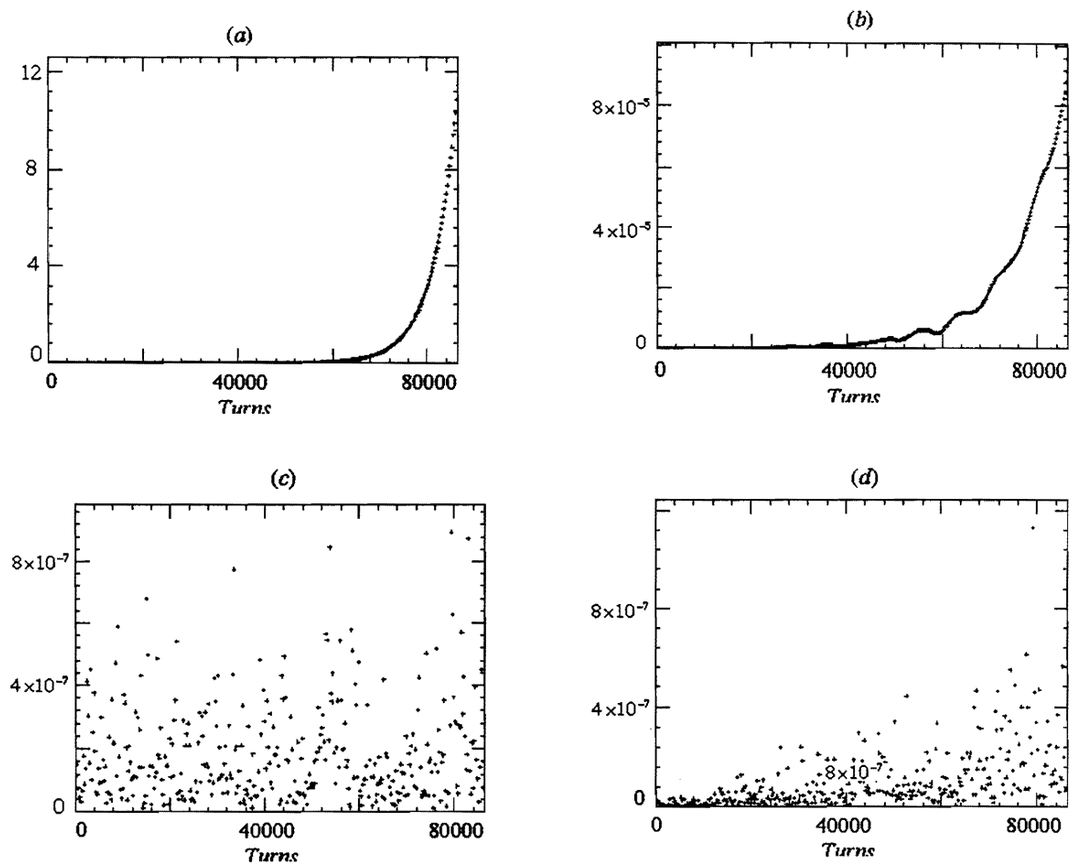

Figure 6: (a) and (b) show horizontal and vertical center-of-mass motions for ξ_o=0.2 and ξ_o=0, respectively. (c) and (d) show horizontal and vertical center-of-mass motions for ξ_o=0.2 and ξ_1=0.2, respectively.

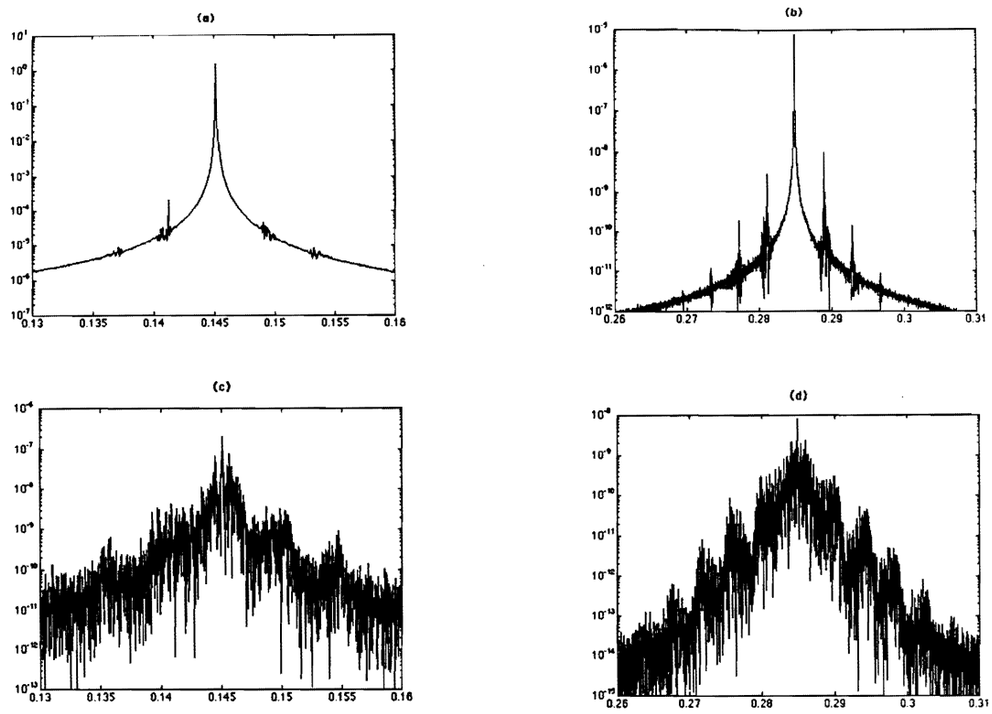

Figure 7: Fast Fourier Transforms of the mean transverse positions of the beam. (a) and (b) show FFT for horizontal and vertical positions of the beam in ξ_o=0.2 and ξ_o=0, respectively. (c) and (d) show FFT for horizontal and vertical positions of the beam in ξ_o=0.2 and ξ_1=0.2, respectively.

References

[1] Eun-San Kim, Simulation of the Longitudinal Instability in ATF Damping Ring, APAC98, (1998).

[2] T. Nakamura, Cure of Transverse Instabilities by Chromaticity Modulation. Proc. 1995 PAC, p.3100

[3] W.H. Cheng, A.M. Sessler, and J. S. Wurtele, Phys. Rev. Lett. 78, 4565 (1997)

[4] K. Bane and K.Oide, Proc. of the 1993 IEEE Particle Acc. Conf., Washington D.C., 1993, p.3339.

[5] R.H. Siemann, Nucl. Instr. and Meth. 221 (1984) 294